Journal of Operational Meteorology
Article

Evaluating Precursor Signals for QLCS Tornado and Higher Impact Straight-Line Wind Events

JUSTIN G. GIBBS
NOAA/National Weather Service, Warning Decision Training Division, Norman, Oklahoma

ABSTRACT

Tornadoes produced by quasi-linear convective systems (QLCS) present a significant challenge to National Weather Service warning operations. Given the speed and scale at which they develop, different methods for tornado warning decision making are required than what traditionally are used for supercell storms. This study evaluates the skill of one of those techniques—the so-called three-ingredients method—and produces new approaches.

The three-ingredients method is found to be reasonably skillful at short lead times, particularly for systems that are clearly linear. From the concepts and science of the three-ingredients method, several new combinations of environmental and radar parameters emerge that appear slightly more skillful, and may prove easier to execute in real time. Similar skill between the emerging methods provides the forecaster with options for what might work best in any given scenario.

A moderate positive correlation with overall wind speed with some radar and environmental variables also is identified. Additionally, mesoscale convective vortices and supercell-like features in QLCS are found to produce tornadoes at a much higher rate than purely linear systems.

---

1. Introduction

Tornadoes produced by quasi-linear convective systems (QLCSs, Weisman and Trapp 2003) present a significant challenge to United States National Weather Service (NWS) warning operations. Statistical evaluation of warning performance suggests tornadoes produced by QLCSs have a lower probability of detection (POD), with more false alarms (Brotzge et al. 2013). Significant (EF2+) QLCS tornadoes also appear to be missed more frequently than for their supercell counterparts (Gibbs and Bowers 2019).

QLCSs have been the subject of extensive research efforts over the years. Initial work first outlined different convective storm modes, airflows, and formations (Browning 1964; Fujita 1978; Smull and Houze 1987; Rotunno et al. 1988). By the 1990s, the more widespread deployment of Doppler radar deepened our insight into features commonly associated with severe weather in linear systems, such as rear-inflow jets and notches (Jorgensen and Smull 1993; Przybylinksi 1995), as well as the rate at which these storms produce tornadoes (Pfost and Gerard 1997; Funk et al. 1999). Through our better understanding of QLCSs we also learned of limitations in convectional approaches to tornado warnings using WSR-88D radars (Trapp et al. 1999).

The 2000s further illuminated storm-scale processes, radar signatures, and environmental conditions associated with straight-line winds and tornadoes. Wakimoto et al. (2006) and Wheatley and Trapp (2008) sharpened our focus on what processes were the most problematic and what radar characteristics signaled those processes. This research led Schaumann and Przybylinksi (2012) to focus on the radar presentation and environmental conditions associated with QLCS tornadoes. The so-called three-ingredients method (hereafter referred to as 3IM) emerged from those efforts.

a. The 3IM for QLCS tornado warning issuance

The 3IM is used by several NWS offices as one technique for issuing QLCS-based tornado warnings

Corresponding author address: Justin Gibbs, 120 David L. Boren Blvd. Ste. 2640, Norman, OK 73071
E-mail: justin.gibbs@noaa.gov

[Warning Decision Training Division (WDTD) 2021]. An infographic (https://rollerwx.files.wordpress.com/2019/01/twip_qlcs_reference_sheets.pdf) shares some of the details of the practice. The 3IM initially focuses on identifying areas of QLCSs associated with a confluence of these three ingredients:

1. a portion of the line where the system cold pool and ambient low-level shear are nearly balanced, or slightly shear dominant,
2. 0–3-km line-normal bulk-shear magnitude >15.43 m s^{-1} (30 kt), and
3. the presence of a rear-inflow jet or outflow causing a surge or bow within the QLCS.

When applying the 3IM, operational meteorologists estimate a line's balance (or shear dominance) by assessing characteristics of radar reflectivity and the line's updraft–downdraft convergence zone. In the example in Fig. 1, the southernmost portion of the line is more parallel to the shear vector, and available buoyancy leads to convection that is roughly balanced with the cold-pool outflow. This is evident by the updraft–downdraft convergence zone aligning closely to updraft towers. Towards the middle of the line, a small area of overhanging precipitation/updraft towers denotes an area where there is slight shear dominance as the line becomes more perpendicular to the shear vector. Farther north—where shear is stronger and buoyancy is lower—larger reflectivity values are embedded in areas of broader stratiform precipitation/updraft towers in a more shear-dominant region of the line. As this example suggests, the subjectivity of this practice can make consistent diagnosis difficult.

The 0–3-km line-normal shear is calculated by finding the component of the 0–3-km shear vector perpendicular to the orientation of the updraft–downdraft convergence zone. Crucially, this can change along the line depending on the shape and local characteristics of the QLCS. Figure 2 presents a line with the focus shifted to the orientation of the updraft–downdraft convergence zone and the 0–3-km shear vector. The leading edge of convection along the white highlighted portion of the line runs roughly parallel to the shear vector, while the portion along the black highlighted section is at a much sharper angle to the overall shear vector. The orientation is such that it results in several local bows and notches that form a nearly 90° angle to the shear vector. The black-dashed portion of the line would experience much higher line-normal shear values. A rear-inflow jet can
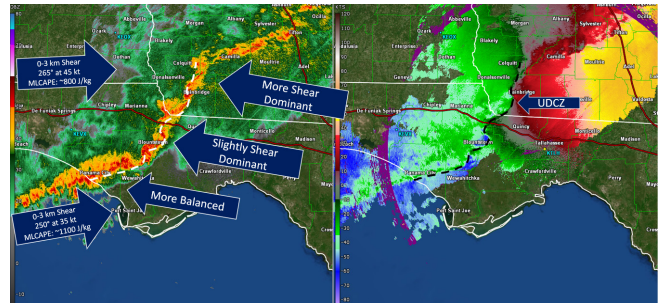

Figure 1. Radar reflectivity (left) and base velocity (right) of a QLCS in the southeastern United States. Arrows indicate points in the line where shear and buoyancy are close to balanced, when the line is slightly shear dominant, and when the line is mostly shear dominant. The white dashed line represents the updraft–downdraft convergence zone on the left image (black dashed on right). The leftmost arrows represent the approximate 0–3-km shear vector and available MLCAPE at the latitude they are aligned. *Click image for an external version; this applies to all figures hereafter.*
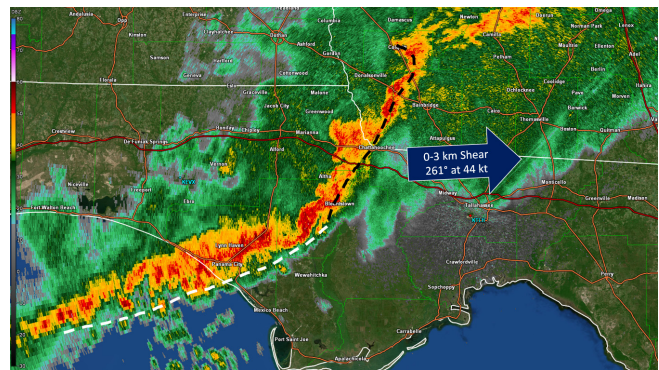

Figure 2. Radar reflectivity of the same QLCS as in Fig. 1. The arrow represents the 0–3-km shear vector's approximate orientation. White dashed lines highlight portions of the updraft/downdraft convergence zone that are more parallel to the shear vector, while black dashed lines represent a section of the line intersecting at a steeper angle.

be identified in radar velocity data, with a broad area of higher velocity values in the area behind the deepest convection (Fig. 3). Care must be applied to not allow radar viewing limitations to mask the velocity data in a well-developed rear-inflow jet.

Once the 3IM criteria are met, several radar signatures are used as "confidence builders" or "nudgers" in anticipating the development of a potentially tornadic mesovortex (Fig. 4). The assertion

of the method is that the more signatures that are present, the higher the probability of tornadic mesovortex formation. The presence of five nudgers is a common threshold for tornado warning decisions after the initial three environmental ingredients are present (WDTD 2021).

These techniques are particularly important because traditional radar velocity characteristics do not provide as much of a precursory signal to QLCS tornado development compared to their supercell counterparts (Trapp et al. 1999; Lyza et al. 2017; Gibbs and Bowers 2019). Additionally, during QLCS post-event surveys, there are considerable challenges in determining the phenomenon that produced damage—straight-line winds or a tornado (Skow and Cogil 2017). The 3IM can help differentiate the locations of these hazards better than previously possible.

This observation-based study takes the elements of the 3IM, WSR-88D velocity rotational characteristics, and additional environmental characteristics known to be associated with QLCS tornado development and examines them for skill in predicting tornado development. The parameters are examined both individually and combined to determine the mix of conditions that are most skillful at short lead times to the onset of QLCS tornadoes. The skill of the 3IM as a pretornadic discriminator also is quantified. The results can be used to refine existing NWS warning methods and decision-making training.

2. Data and methods

a. Case selection

Data were sought from QLCSs that could plausibly prompt severe thunderstorm and/or tornado warning decisions. The Storm Prediction Center (SPC) severe weather event archive (https://www.spc.noaa.gov/exper/archive/events/) provided an avenue to examine events using the report and mesoanalysis archive. Events from November 2018 to July 2020 were evaluated for inclusion into this study if they met the following criteria:

1. >5 severe wind reports,

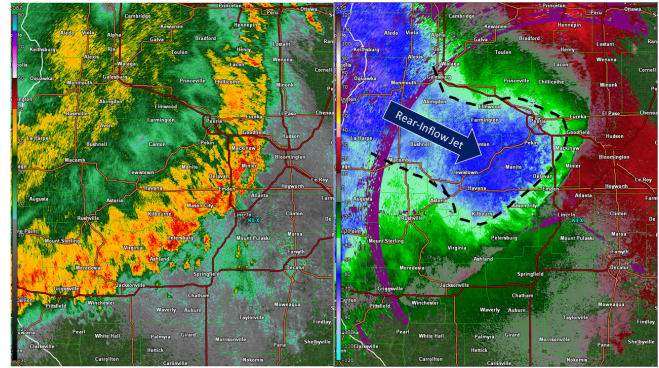2. a linear presentation on radar along the lines identified by Smith et al. (2012),

Figure 3. Radar reflectivity (left) and base velocity (right) for a QLCS with a well-sampled rear-inflow jet. The arrow sits along the best sampled axis of the jet, with the black dashed lines outlining the strongest apparent velocities.
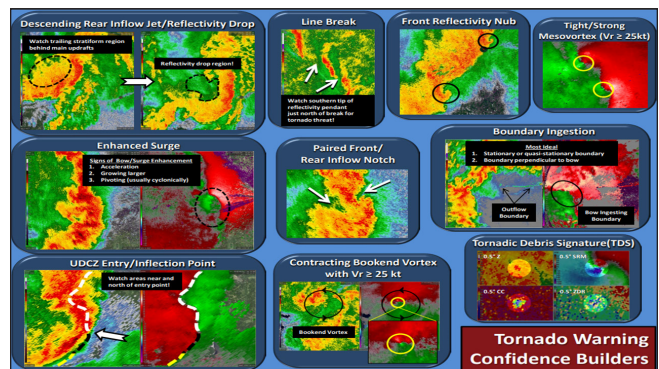

Figure 4. Infographic of confidence builders used as warning indicators in the three-ingredients method (3IM).

3. effective bulk shear >12.86 m s^{-1} (25 kt) along the line (evaluated from the SPC mesoanalysis archive to ensure semi-organized convection), and

4. ≤166.68 km (90 n mi) from a WSR-88D site (because sampling height and resolution limitations beyond this distance make many of the features difficult or impossible to observe).

Once a candidate event was identified, relevant WSR-88D data were downloaded from the National Centers for Environmental Information level II radar archive (https://www.ncdc.noaa.gov/nexradinv/) and viewed using GR2Analyst version 2.80.

Efforts were focused on capturing a spectrum of QLCS events, while attempting to avoid oversampling a single QLCS in time and space. Therefore, once a

sample was collected from a QLCS event, another sample could not be taken within 80.46 km (50 mi) of that point for at least one hour. In order to better capture stronger and rarer features in a system, priority was given to samples based on the following characteristics (in order):

1. confirmed tornadoes,

2. areas of nontornadic wind damage [estimated or measured gusts ≥35.76 m s⁻¹ (80 mph), and

3. areas of nontornadic wind damage [estimated or measured gusts ≥25.92 m s⁻¹ (58 mph)].

This prioritization meant that a stronger report took precedence and defined the 1-h, 80.46-km (50-mi) buffer (i.e., all lower reports would not be collected during that time, within that radius). However, reports were always able to be collected outside of the 80.46-km (50-mi) radius. Tornado occurrence and straight-line wind speeds were determined by NWS storm surveys and storm reports. This comes with the obvious caveat to the limitations of storm surveying, damage reporting, and available damage indictors.

Figure 5 gives an example of the process. A tornado sample was taken near the tornado label at 1910 UTC, and 80.46 km (50 mi) away a damaging wind sample was collected. No other samples were taken from this line until 2010 UTC when one tornado sample was taken for a new tornado that had occurred. In this example, other wind damage occurred to the south of the tornado at nearly the same time, but none of the reports were located >80.46 km (50 mi) from this tornado so the wind damage reports would not have been included in the database.

These methods produced a database of 400 samples from 74 different severe weather episodes. One hundred seventy-two tornado events were sampled, ranging in intensity from EF0 to EF4. One hundred ninety-seven of the 400 total sampled cases produced winds estimated by NWS storm reports ≥35.76 m s⁻¹ (80 mph; both tornadic and nontornadic). Figure 6 shows the geographic distribution of each of these 400 cases, with the season in which they occurred. Spring (MAM) produced 30 events; summer (JJA) produced 32 events; winter (NDJF) produced 11 events; and fall (SO) produced 2 events. The cases cluster in a few locations where multiple QLCS events occurred, but they have a reasonable geographic diversity.
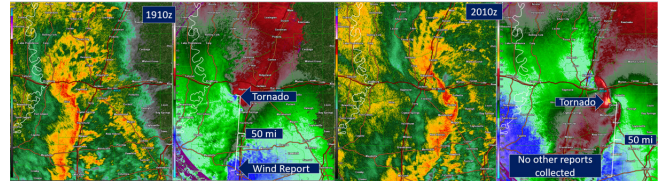

Figure 5. An example of the sampling methods used in the study. The leftmost radar and radar velocity combination is from 1910 UTC, where the rightmost is from 2010 UTC. The Tornado label on the left and right image indicates where two tornado samples were taken one hour apart. The white bracket displays approxmiately 80.46 km (50 mi) of separation. The wind report label shows where a wind report was taken from 1910 UTC. While there were other wind reports within 80.46 km (50 mi) of the 2010 UTC tornado report, none occurred >80.46 km (50 mi) away, therefore no other reports met the separation criterion to be included in the database.
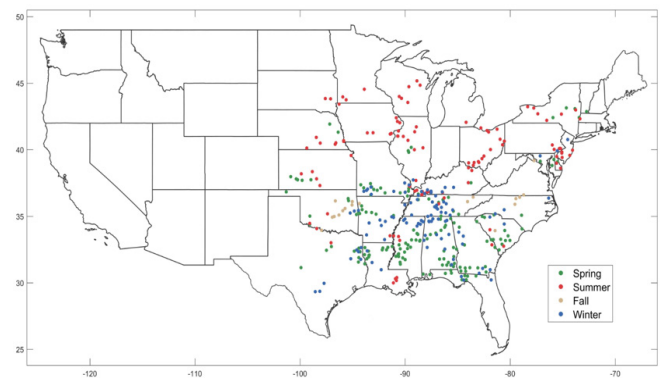

Figure 6. A plot of the approximate location of each event entered into the database for this study. Green dots are cases from March to May, red from June to August, brown from September to October, and blue November to February. The x axis is degrees longitutde and the y axis is degrees latitude. Map prepared in Matlab by Katy Christian from WDTD.

b. Adjustments to the original 3IM approach

Three adjustments were made to the 3IM for this study. First, 0–3-km CAPE was calculated both as a nudger and as a separate environmental parameter. The second adjustment was consolidating the confidence builders and nudgers into the 11 most distinct features—hereafter referred to as linear tornado indicators (LTIs). Each LTI was collected in the final volume scan prior to the onset of damage. Figure 7 shows examples of the first six indicators. The LTIs are:

- a descending rear-inflow jet (DRIJ), characterized by enhanced velocity values coupled with lower values of reflectivity in the rear of the storm, suggesting subsidence (Fig. 7a); these values also can be evaluated using the full volume scan on cross sections;
- a line break in the 50-dBZ reflectivity along the updraft–downdraft convergence zone (Fig. 7b);
- a front reflectivity notch, which is a surge in higher reflectivity values ahead of the updraft–downdraft convergence zone and main area of higher reflectivity (Fig. 7c);
- an enhanced surge or bow echo (Fig. 7d); these were counted both for larger mesoscale bow-echo features and smaller storm-scale elements;
- the ingestion of small-scale boundaries visible in reflectivity, often a result of outflow from nearby convection (Fig. 7e);
- a paired inflow notch—with a clear weak-echo region embedded into the line with a velocity signature coupled with the notch—suggesting strong local inflow (Fig. 7f);
- the presence of mesovorticies with rotational velocity (Vrot) ≥ 10 m s^{-1} (20 kt) and bookend vortices located at the edge of larger linear features; note that this indicator relaxes the mesovortex criterion in the original 3IM slightly and removes the requirement of a contracting bookend vortex, which would be challenging to quantify in real time; in keeping with the original 3IM, the presence of a bookend vortex counted as two indicators—both as a mesovortex and as a bookend mesovortex;
- a "reflectivity tag" intersecting the line for including apparent surges within reflectivity products that were intersecting the line nearly perpendicularly; an example can be seen online (https://training.weather.gov/wdtd/temp/justin/acceleration-tag/story_html5.html);
- cell mergers occurring within the line; and
- a history of tornado production within the past hour.

The third adjustment to the 3IM approach was that a tornadic debris signature (TDS) was not included as an LTI. This was removed as an active TDS signifies an ongoing tornado—not something that could be used as a pre-event warning indicator.
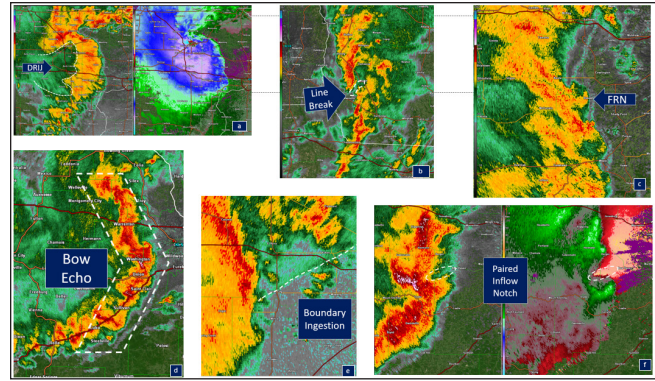

Figure 7. The first six (a–f) linear tornado warning indicators documented in the study. White dashed lines outline features of interest in each panel. FRN refers to front reflectivity nub in (c). Click on each link below for a larger image: a, b, c, d, e, f.

c. *Storm-specific data*

In addition to the modified 3IM elements, Table 1 lists additional data that were collected for each event at the final volume scan preceding tornadogenesis (or wind damage for nontornadic storms). Because velocity features are easier to measure objectively, Vrot, mesocyclone diameter, and mesocyclone depth also were collected one additional volume scan prior to onset.

Trends from preceding volume scans were used, when necessary, to confirm the LTI features present at the final volume scan. This made it difficult to test for these features definitively at earlier scans. Rotational data and mesocyclone depth were only included if one met the criterion of Vrot ≥ 10 m s^{-1} (20 kt); otherwise, it was set to zero. In the event of multiple circulations, the one that appeared to best match the location of the damage/tornado event was used. Supplemental 0.5° cuts (i.e., SAILS) were not included because of potential inconsistencies in usage that might result in significant differences between collection time from case to case.

Table 2 lists the environmental parameters collected from the SPC 40-km mesoanalysis archive for each event using the analysis from the hour before the event occurred. Manual adjustments were made to 12 cases in which the automated archive produced values unrepresentative of the storm inflow (missing data, convective contamination, etc.). From the database of environmental data, the following were then calculated for each event based on the existing information:

Table 1. A list of storm-specific and radar-based characteristics collected for each storm within the volume scan prior to each event; radar rotation characteristics also were collected for the second to last volume scan.

Storm/Radar Characteristics Examined Beyond 3IM	
Latitude, Longitude and Time of Each Event	Range from nearest WSR-88D (nm)
V_{rot} above 10.28 m s^{-1} (20 kt) and distance between Vmax and V_{min} (Burgess et al. 1993)	Cell characteristics (MCV, Supercell-like, etc.)
Volumetric Peak Rotational Speed of the Circulation (RSC) (Gibbs and Bowers 2019)	Storm motion/speed (based on UDCZ geometry)
Meso depth (above 10.28 m s^{-1}; 20 kt Vrot) (Burgess et al. 1993)	Estimated peak wind per survey or LSR
Damage location (front/middle/rear of cell)	Tornado Y/N and EF rating

Table 2. Environmental variables collected from each event from the SPC 40-km meosanalysis archive.

Environmental Variables Collected	
100 hPa mixed layer CAPE (J kg^{-1}) (Thompson et al. 2012)	100 hPa mixed layer CIN (J kg^{-1}) (Thompson et al. 2012)
Mixed Layer LCL Height (m) (Thompson et al. 2012)	Downdraft CAPE (J kg^{-1}) Gilmore and Wicker 1998
Surface Mixing Ratio (g/kg) (Holton 2004)	0–3-km CAPE (J kg^{-1}) (Thompson et al. 2012)
0–6, 0–3, 0–1-km Shear Magnitude and Direction (Rasmussen and Blanchard 1998)	0–6, 0–3, 0^{-1} Storm Relative Helicity (Rasmussen and Blanchard 1998)
Significant Tornado Parameter (Thompson et al. 2012)	500–700 and 500–850 hPa Environmental Lapse Rate (°C km^{-1}) (Holton 2004)

- 0–6-, 0–3- 0–1-km line-normal shear (hereafter referred to as 06LN, 03LN and 01LN, respectively); this equals shear magnitude × cos(|line orientation angle – shear direction angle|); and
- rotational speed of the circulation (RSC) with normalized mesocyclone depth (RMD); this equals RSC × [(height of mesocyclone – base of mesocyclone)/1000].

d. Storm mode sub-taxonomy

QLCS tornado events take on a variety of appearances and sub-morphologies. After initial case collection, three features were noted to have appeared most often. This led to each of the 400 cases being subdivided further. Here are the results:

- 52 mesoscale convective vortex (MCV) events (Houze 2004);
- 12 "super QLCS" events displaying supercell-like characteristics during tornado production, while having displayed linear characteristics ≤30 min before the tornado; and
- 336 true linear events—did not exhibit MCV or super QLCS characteristics.

An example of a true linear event can be seen in Fig. 8. The low-level reflectivity maintains a persistent 45–50-dBZ continuity along a continuous updraft–downdraft convergence zone in velocity. Reflectivity aloft also maintains some general continuity; there are local maxima and minima, but an overall radar appearance supports one continuous system.

Figure 9 shows an example of an event classified as an MCV, with a distinct S-shape in reflectivity, and local velocity maxima surrounding a central circulation. These systems often produced circulations at locations other than the leading edge of advancing 50+ dBZ reflectivity and occurred in shear-dominant areas of convection.

Figure 10 shows the transition of what initially appears to be a mostly linear system into what has been classified as a super QLCS. The convection initially manifests itself as a line, with local indicators, and then develops a clear supercell signature with deep and persistent rotation. A weak-echo region is apparent aloft, and at the lowest elevation angle there is a hook echo collocated with a vigorous sweeping velocity couplet with Vrot >36 m s^{-1} (70 kt). An example animation can be found online (https://training.weather.gov/wdtd/temp/justin/super-qlcs/story_html5.html).
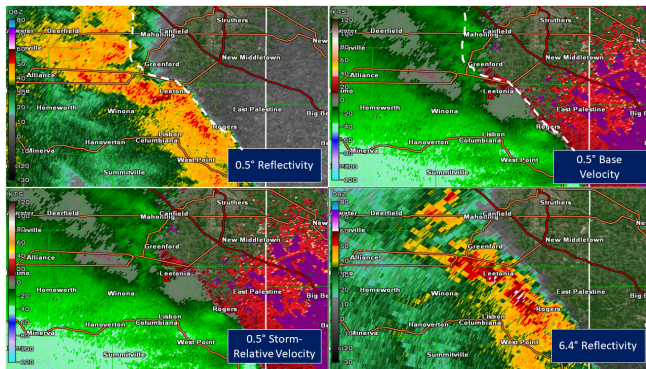
Figure 8. An example of the type of event determined to be truely linear within the database of selected events. The top left is 0.5° reflectivity, top right 0.5° base velocity, bottom left 0.5° storm-relative velocity (set perpendicular to the leading edge of the line), and the bottom right 6.4° reflectivity. The white dashed lines represents the approximate location of the updraft–downdraft convergence zone.
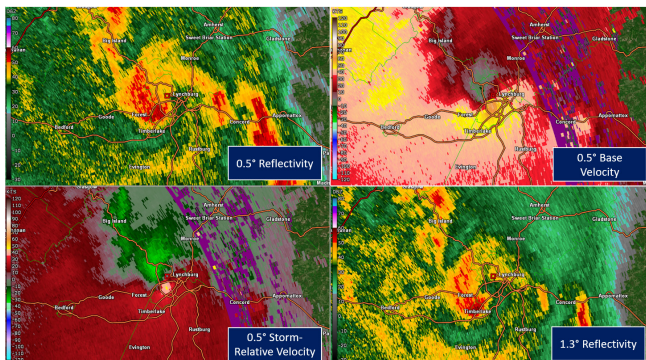

Figure 9. An example of a case classified as a mesoscale convective vortex (MCV). Data moments are the same as Fig. 8, except the reflectivity in the bottom right panel is at 3.4°.

e.   Data analysis methods

Data were first analyzed for skill in determining tornadic versus nontornadic damage using the 3IM. Skill was assessed using POD, false alarm ratio (FAR), critical success index (CSI, Schaefer 1990), and Heidke skill score (HSS, Heidke 1926). Skill was calculated for the presence of the three primary ingredients and different numbers of LTIs (3–7) as a warning threshold.

A database of 35 radar/storm-based variables and 17 environmental variables remained. A variety of combinations of these variables were then examined, such as individual LTIs in 01LN conditions, number of LTIs multiplied by shear conditions, and other environmental variable combinations with radar
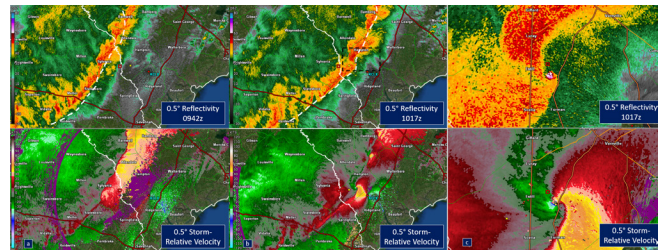

Figure 10. (a, left) An example of mostly linear convection at 0942 UTC prior to the appearance of clear supercell characteristics. Data moments are 0.5° reflectivity and storm-relative velocity. The white dotted lines represent the updraft–downdraft convergence zone. (b, center) The same moments as in (a) but at 1017 UTC. The black dashed box highlights the approximate region contained in the right column. (c, right) Zoomed image of panel (b) showing clear supercell characteristics with a weak-echo region/inflow notch, sweeping velocity couplet, and hook echo with embedded 70+ dBZ reflectivity (suggestive of debris). Click on each link below for an expanded version that includes reflectivity aloft to provide context for the updraft characteristics: a, b, c.

permutations. RStudio was used to create correlation matrices to determine potential statistically significant combinations. Pearson's correlation coefficient values were utilized between whether a tornado occurred (1 for yes, 0 for no) and for overall wind speed. Parameters that showed a correlation coefficient >0.250 were added to a list for skill testing. Once the list of parameters was developed, each parameter had thresholds tested for use as a warning threshold. This was done using POD, FAR, CSI, and HSS metrics and box-and-whisker and violin plots in RStudio. These metrics then were used to further refine optimal thresholds. This was done for all cases, and then separately for true linear, MCV, super QLCS, and MCV and super QLCS combinations (hereafter referred to as special cases). For the MCV subtype, skill was assessed at differentiating tornadic versus nontornadic events. Additionally, analyses were done that compared parameters to see which ones identified "special case" events out of the larger dataset. Calculations also were made for cases within 74 km (40 n mi) of the sampling WSR-88D. The selection of 74 km was somewhat arbitrary, but for this dataset resulted in an approximately equal number of cases inside and outside of that range.

3. Case study demonstration

a. *Skill scores for the modified 3IM*

A primary motivation for this study was to objectively evaluate the skill of the 3IM for making tornado warning decisions. This method has emerged in usage across the NWS, and formal training has been introduced by WDTD, yet to date neither the method nor its verification data have been published in the refereed literature. The hypothesis from the operational use of the 3IM is that tornadoes will occur more frequently when more LTIs are present (Schaumann and Przybylinski 2012).

The combination of the three ingredients from the 3IM and five LTIs (hereafter 3IM+5) was the most skillful differentiating between tornadic and nontornadic storms. The skill was highest for true linear events—removing MCV and super QLCS events. Table 3 shows the skill of the method as a tornado warning threshold. The skill was roughly equal to the 2017–2019 tornado warning skill average for POD based on the NWS Performance Management database (https://verification.nws.noaa.gov/), but displayed a lower FAR. A commonly observed detection failure was that the tornado occurred in a more shear-dominant portion of the line (40 times in the database), rather than near a balanced, or slightly shear-dominant portion of the updraft–downdraft convergence zone. There also were a few instances where tornadoes occurred when the 03LN was slightly less than the 3IM threshold of 15.43 m s^{-1} (30 kt).

b. *Other skillful tornadic storm discriminators*

Different mathematical combinations of environmental thresholds and/or radar rotational characteristics provided a foundation to explore for skillful metrics. This was particularly true of line-normalized shear values multiplied by the number of LTIs present. Certain radar rotational characteristics also appeared skillful when multiplied by shear parameters. Tables 4 and 5 show an initial selection of parameters that were multiplied by LTI to produce a skillful tornado warning discrimination. RMD, when multiplied by 01LN, was the most skillful with a threshold of 10 000, with the remainder of parameters showing lower, but similar skill. Figure 11 present tornadic and nontornadic case values between two parameters that showed similar warning skill (1/LCL Height × 01LN × LTI and 01LN
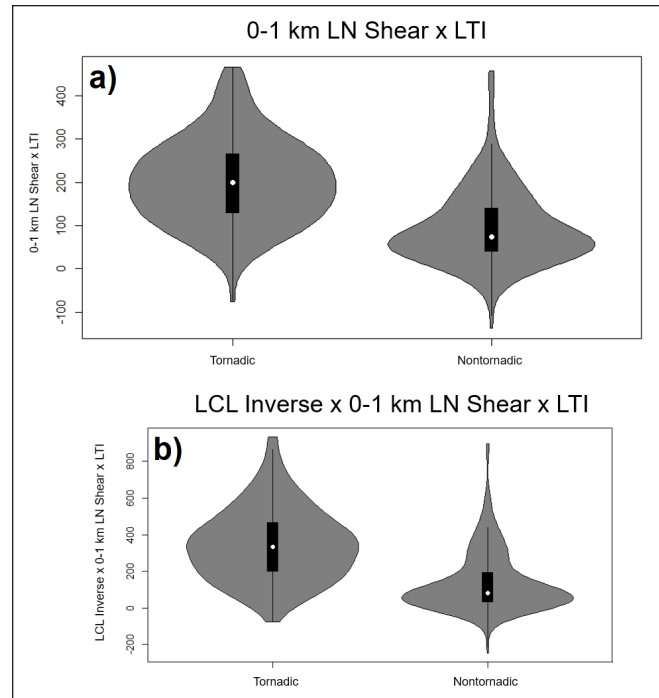

Figure 11. Violin plots, with embedded box-and-whisker plots, of tornadic and nontornadic cases (abscissa) for (a) 01LN × nudgers and (b) LCL inverse × 01LN × nudgers.

× LTI). There is noteworthy separation between the two parameters regarding tornadic and nontornadic storms.

Several parameters relied on different objective and subjective measurements to discriminate QLCS tornadoes. Table 6 shows these parameters, and their CSI values separated by all events, and only events inside 74 km (40 n mi), where presumably low-level rotation and reflectivity signatures would be more likely to be detected. Two key takeaways emerge from these data. First, the 3IM is more skillful with true linear events and most skillful within 74 km (40 n mi) of the radar. Second, the other parameters have similar skill to one another, with expected improvements inside of 74 km (40 n mi). Many also demonstrate slight improvements to 3IM+5. This provides the forecaster options in choosing a suitable method.

To be the most precise, RMD × LTI × 01LN with a threshold of 10 000 produces CSI >0.600 in all situations. However, this may prove unwieldy in a warning environment, and probably serves best as a conceptual model (i.e., the deepest, strongest rotating storms with the most LTIs present in the best shear environment are the most likely to produce tornadoes).

More simply, forecasters could count the number of LTIs and multiply that by 01LN (with a warning

Table 3. Skill scores of the 3IM and 5 LTI as a tornado warning threshold as compared to the national baseline for tornado warnings from June 2017 to June 2020. Available online at https://verification.nws.noaa.gov/.

Three-Ingredients Method and 5 LTI (3IM+5) as a tornado warning threshold			
	All Cases	**True Linear**	**National Baseline TOR Skill (2017–2020)**
POD	0.585	0.616	0.607
FAR	0.411	0.426	0.695
CSI	0.376	0.422	0.254
HSS	0.200	0.236	NA

Table 4. Skill scores of combinations of environmental and radar rotational parameters with LTI as a tornado warning threshold. The threshold when calcluated using kt and n mi is given in italics. The same format applies to each table hereafter.

Skill of Environmental and Radar Rotational Characteristics multiplied with LTI as a Tornado Warning Threshold – All Events					
	01LN × LTI	**03LN × LTI**	**0–1-km SRH × LTI**	**0–3-km SRH × LTI**	**V_{rot} × LTI**
Threshold	*150*	*225*	*225*	*2000*	*200*
POD	0.680	0.697	0.678	0.672	0.751
FAR	0.319	0.329	0.245	0.304	0.304
CSI	0.515	0.519	0.556	0.519	0.565
HSS	0.301	0.304	0.327	0.304	0.327

Table 5. Additional environmental and radar rotational parameters with threshold and skill score information.

Skill of Environmental and Radar Rotational Characteristics coupled with LTI as a Tornado Warning Threshold – All Events			
	RMD × LTI	**RMD × LTI × 01LN**	**Inverse LCL Height × 01LN × LTI**
Threshold	*1200*	*10000*	*175*
POD	0.789	0.704	0.744
FAR	0.389	0.099	0.344
CSI	0.525	0.654	0.535
HSS	0.304	0.385	0.305

threshold of 150), or else use Vrot multiplied by LTIs (with a threshold of 200). Both approaches produce CSIs >0.500, with the Vrot approach >0.600 inside of 74 km (40 n mi).

Identifying LTIs is subjective, and forecasters who prefer more concrete datasets could utilize Vrot multiplied by 01LN with a threshold of 300, although this method dips below 0.500 CSI in true linear events. Another option would be RMD × 01LN with a threshold of 5000, which is somewhat more skillful, yet more cumbersome to calculate. The existence of a mesovortex with Vrot $\geq$10 m s^{-1} (20 kt) in a 01LN environment of $\geq$12.8 m s^{-1} (25 kt) also produces a CSI >0.400.

The original 3IM also likely can be employed with reasonable proficiency, particularly in true-linear events, if forecasters feel more comfortable with this approach. Skill scores were slightly lower, but these tests were strictly yes/no for shear parameter thresholds and LTI presence. The inherent subjectivity of the original 3IM might serve experienced forecasters well when conditions/LTIs are more marginal or ground-truth appears to be outperforming or underperforming expectations.

Surprisingly, MLCAPE, MLCIN, DCAPE, surface mixing ratio, 0–3-km MLCAPE, effective significant tornado parameter, and 700–500- and 850–500-hPa lapse rates were not able to be combined to discriminate

Table 6. Skill scores of provided parameters as a tornado warning threshold. Events with a $^{-1}$ are from two volume scans prior to the onset of damage, or a tornado. Events without this notation are from the final volume scan prior to the event.

Skill of parameters as a tornado warning threshold					
Parameter	Threshold	All Events	True Linear	All Inside 74 km (40 n mi)	True Linear Inside 74 km (40 n mi)
01LN × LTI	150	0.515	0.569	0.535	0.424
03LN × LTI	200	0.530	0.452	0.500	0.420
3IM+5	N/A	0.376	0.422	0.477	0.470
Vrot × LTI	200	0.565	0.554	0.617	0.630
Vrot^{-1} × LTI	200	0.542	0.562	0.550	0.586
RSC × 01 LN SRH	500	0.570	0.531	0.572	0.572
RMD × LTI	750	0.601	0.559	0.635	0.540
RMD^{-1} × LTI	750	0.552	0.549	0.560	0.531
Vrot × 01LN	300	0.547	0.502	0.585	0.524
Vrot^{-1} × 01LN	300	0.532	0.462	0.524	0.550
Meso × 01LN	25	0.530	0.440	0.533	0.460
RMD × 01LN	5 000	0.547	0.500	0.640	0.534
RMD^{-1} × 01LN	5 000	0.539	0.484	0.564	0.526
(01LN + 03CAPE) × LTI	500	0.423	0.423	0.518	0.407
RMD × LTI × 01LN	10 000	0.654	0.617	0.676	0.651
RMD^{-1} × LTI × 01LN	10 000	0.616	0.565	0.588	0.577

as well between tornadic and nontornadic storms in multiple configurations/permutations (e.g., MLCAPE × 0–3-km CAPE × LTI, etc.). Even when these less-skillful parameters were combined with shear and thermodynamic variables that were skillful, the skill was worse or had no significant change (e.g., MLCAPE × 01LN × LTI). This may allow the forecaster to focus more on parameters like 01LN, assuming sufficient MLCAPE is present to produce deep convection.

Tests also were conducted using 0–3-km MLCAPE as a traditional LTI, consistent with the original 3IM. Skill scores were virtually identical when including it as a LTI (CSI = 0.378) and slightly worse than other combinations when factoring it in to multiple environmental calculations (e.g., 01LN × 0–3-km MLCAPE × LTI; CSI = 0.458). These results seem to suggest that including 0–3-km MLCAPE >40 J kg^{-1} as an LTI does not appear to add much, if anything, to tornado warning skill.

c. Pretornadic intensity estimation

Among QLCS events that produced tornadoes, it was more difficult to find clear precursor indications of systems that would produce stronger tornadoes. Most of the above-mentioned techniques showed little correlation or failed to present a good threshold of significance for differentiating between, for example, tornadoes that produced a peak estimated wind speed above or below 46.9 m s^{-1} (105 mph). The combination that showed the best correlation was as follows: MULTI = 01LN × 03LN × 06LN × (1/LCL height) × MLCAPE.

Figure 12 shows a plot of peak wind speed with the MULTI parameter (correlation coefficient = 0.359), with higher values correlating to higher wind speeds in tornado events. This weak correlation follows the expected result that the combination of low-level and deep-layer shear with instability and local acceleration indication via LTI might be a precursor for stronger tornadoes. A lack of pretornadic strength clues contrasts to recent work in supercell intensity focused on various rotational characteristics and mesocyclone width that
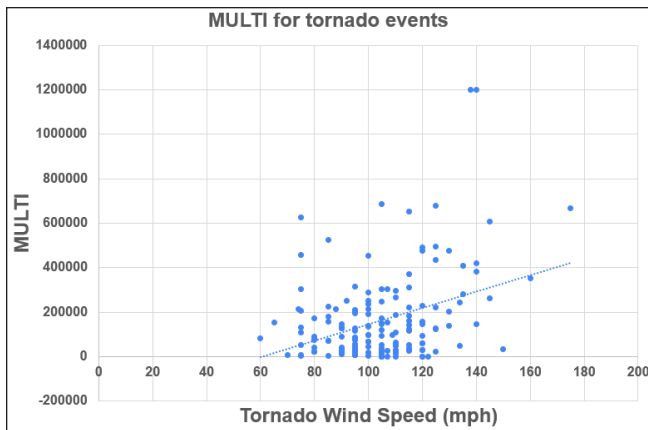
Figure 12. Scatter plot of the MULTI parameter across tornadic events. The x axis is the events peak wind speed, the y axis the value of the MULTI parameter, and the dotted line is a linear trendline (R = 0.359, R2 = 0.1291).

showed strong correlation to final intensity (Gibbs and Bowers 2019; Sessa and Trapp 2020). This may be partially a result of the narrower range of final QLCS intensity, as well as the uncertainties in final QLCS tornado intensity owing to surrounding wind damage (Skow and Cogil 2017). Marion and Trapp (2021) found a stronger correlation between pretornadic QLCS mesocyclone width and final tornado intensity.

d. Special cases

The MCV and super QLCS special cases produced tornadoes at a much higher rate than true linear situations. Fifty-two of the 64 identified special cases (81%) were associated with tornadoes, as opposed to 121 out of 336 true linear events (36%). These events also tended to be stronger, with a mean surveyed intensity of 54.1 m s^{-1} (121 mph)—compared to 44.7 m s^{-1} (100 mph) for true linear tornado events. There were not enough nontornadic special cases to examine environmental/radar differences between tornadic and nontornadic storms within that subset, with any confidence. Environmentally, 01LN showed the best differentiation between true linear, MCV, and super QLCS cases (Fig. 13). Future work that identifies precursor characteristics for MCV and super QLCS cases may prove operationally valuable given their apparent propensity to produce tornadoes. The high rate of observed tornado production also may have been a result of the sampling methods of this study (tornadoes and wind damage were sought out and not MCV and super QLCS features). Future work specifically
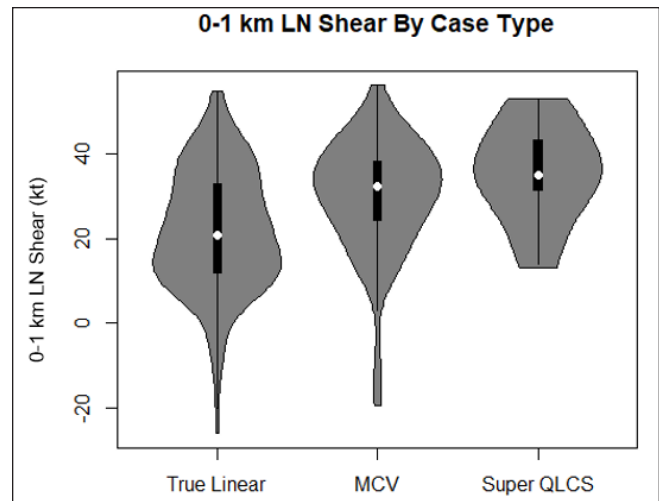

Figure 13. Violin plots with embedded box-and-whisker plots for 01LN stratified by true linear, MCV, and super QLCS events.

examining MCV and super QLCS features and then assessing tornado production would likely prove insightful.

e. Overall wind speed discrimination

Across all cases there were a few parameters that had somewhat higher correlations with overall peak wind speed, regardless of whether the storms were tornadic. Specifically, 01LN × LTI showed the strongest correlation at 0.517 (Fig. 14). Similar correlations existed for 03LN × LTI, as well as 01LN, 03LN, and 06LN with MLCAPE and LTI. For true linear cases, the correlation was slightly stronger at 0.541. In contrast to tornado-producing cases, the introduction of LCL height to this calculation weakened the correlation. The depth of the pre-event mesocyclone at one and two volume scans prior to damage also showed a moderate correlation to peak wind speed, at 0.436 and 0.501, respectively.

f. Caveats and limitations

Perhaps the most significant limitation to many of these methods is the inherent subjectivity of identifying the LTIs. Different signals will appear with varying degrees of clarity and two forecasters might interpret the same data differently. Because of the need to identify relatively small reflectivity and velocity features, these tests also were limited to inside of the 167-km (90 n mi) range from the nearest WSR-88D, and the data showed that many of the techniques had higher
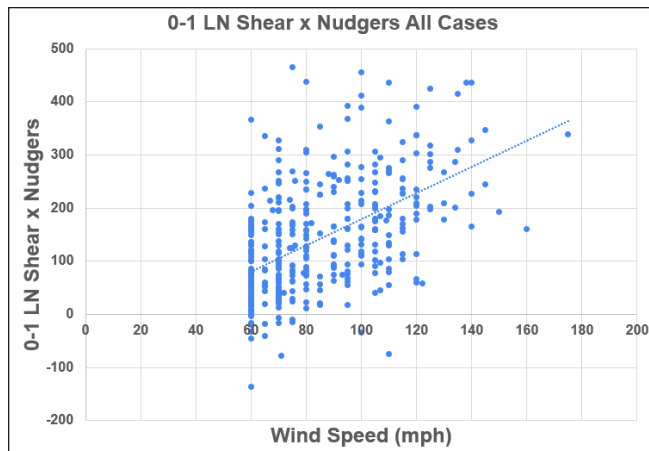
Figure 14. Same as Fig. 12 except for 01LN × nudgers in all cases with the x axis representing total event wind speed and the y axis indicating the value of 01LN × nudgers. $R = 0.529$ and $R^2 = 0.2807$.

accuracy inside of 74 km (40 n mi). Importantly, these tests were conducted at very short lead time—at one and two volume scans prior to tornado development. Further work will be needed to see if the techniques work at longer lead times that more closely match tornado warning performance goals.

Whereas the dataset likely was sufficiently large to determine general takeaways, it was collected from a broad swath of the country, and seasonal and regional variations in QLCS tendencies may not be well represented. Limitations in damage reporting, surveying, and available damage indicators also may be masking the true intensity of some of the events in the database.

Finally, although these methods appear to be more skillful than current tornado warning verification, they do not detect all events and do create false alarms, just as any existing tornado warning strategy does. Warning thresholds will likely serve better as guides than as objective rules, and forecasters should always leverage their experience and all available tools in a QLCS tornado warning environment.

4. Conclusions

The results provide the first formal quantification of skill of the 3IM for QLCS tornado prediction, finding it reasonably skillful and offering some minor modifications. The 3IM skill improves when MCV and super QLCS cases are removed. However, other combinations of radar and environmental parameters may provide slightly more skill, with a simpler approach.

A variety of combinations provided similar skill, but the ones likely to be the most useful to operational meteorologists include 01LN × LTI, with a warning threshold of 150, or $V_{rot} \times$ LTI, with a warning threshold of 200. If forecasters prefer to avoid the subjectivity of LTIs, $V_{rot} \times$ 01LN with at threshold of 300, or the presence of a mesocyclone with $V_{rot} >$10 m s^{-1} (20 kt) in a 01LN environment $\geq$12.8 m s^{-1} (25 kt) performs similarly. The highest skill involves RMD × LTI × 01LN with a threshold of 10 000. However, this may prove too cumbersome for operations, and the conceptual model of stronger/deeper rotation in stronger 01LN environments with more LTIs being a more favorable tornado signal may be more useful than trying to quantify these values.

Super QLCS events (described as linear events that quickly developed supercell characteristics) and MCV events produced tornadoes at a much higher rate than events that only displayed linear characteristics. These tornadoes also tended to be somewhat stronger than their true linear system counterparts. Even though precursor signals for MCVs and super QLCS events were not directly identified in this study, they tended to occur in areas of modestly (but consistently) stronger 01LN.

There also was a moderate positive correlation between the 01LN × LTI and peak overall wind speed in QLCSs, regardless of whether a tornado was produced. Tornado peak wind speed was more challenging, but a mixture of low-level and deep-layer shear, coupled with LCL height and MLCAPE, provided the best (if weak) correlation to tornado peak intensity.

All tests were conducted at very short lead time. Future work should include earlier precursor volume scans to determine how far in advance the signals are detectable. Dual-polarization variables may provide additional indicators, although examination of the initial cases involved in this study found no discernable signals. An examination of precursor signals for MCV and super QLCS events also may help with tornado detection given their tendency (among this dataset) to produce tornadoes.

Hardy for their helpful internal reviews. Thanks to the team at the WDTD for supporting my exploration of this topic while managing other tasks. Thanks to JOM Editor Dr. Katie Wilson, Dr. Jeff Trapp, and two anonymous reviewers whose feedback greatly improved the manuscript. Thanks to my wife Cindy for keeping our kids safe and happy during the day allowing me to work during the COVID-19 pandemic, and thanks to Caleb and Kailey for providing a great reason to keep working through all this. This project was mostly completed amid their playful chaos during pandemic telework, except for the part completed in my parents' basement.

————————————————

REFERENCES

Brotzge, J. A., S. E. Nelson, R. L. Thompson, and B. T. Smith, 2013: Tornado probability of detection and lead time as a function of convective mode and environmental parameters. *Wea. Forecasting*, **28**, 1261–1276, Crossref.

Browning, K. A., 1964: Airflow and precipitation trajectories within severe local storms which travel to the right of the winds. *J. Atmos. Sci*., **21**, 634–639, Crossref.

Burgess, D. W., R. J. Donaldson Jr., and P. R. Desrochers, 1993: Tornado detection and warning by radar. *The Tornado: Its Structure, Dynamics, Prediction, and Hazards, Geophys. Monogr*., No. 79, Amer. Geophys. Union, 203–221.

Fujita, T. T., 1978: Manual of downburst identification for project NIMROD. Satellite and Mesometeorology Research Paper 156, University of Chicago, Dept. of Geophysical Sciences, 104 pp. [Available online at https://swco-ir.tdl.org/bitstream/handle/10605/261961/ttu_fujita_000220.pdf.]

Funk, T. W., K. E. Darmofal, J. D. Kirkpatrick, V. L. DeWald, R. W. Przybylinski, G. K. Schmocker, and Y.-J. Lin, 1999: Storm reflectivity and mesocyclone evolution associated with the 15 April 1994 squall line over Kentucky and southern Indiana. *Wea. Forecasting*, **14**, 976–993, Crossref.

Gibbs, J. G., and B. R. Bowers, 2019: Techniques and thresholds of significance for using WSR-88D velocity data to anticipate significant tornadoes. *J. Operational Meteor*., **7** (9), 117–137, Crossref.

Gilmore, M. S., and L. J. Wicker, 1998: The influence of midtropospheric dryness on supercell morphology and evolution. *Wea. Forecasting*, **126**, 943–958, Crossref.

Heidke, P., 1926: Calculation of the success and goodness of strong wind forecasts in the storm warning service. *Geogr. Ann*., **8**, 301–349, Crossref.

Holton, J. R., 2004: *Introduction to Dynamic Meteorology*. 4th ed. Academic Press, 501 pp.

Houze, R. A., Jr., 2004: Mesoscale convective systems. *Rev. Geophys*., **42**, RG4003, Crossref.

Jorgensen, D. P., and B. F. Smull, 1993: Mesovortex circulations seen by airborne Doppler radar within a bow-echo mesoscale convective system. *Bull. Amer. Meteor. Soc*., **74**, 2146–2157, Crossref.

Lyza, A. W., A. W. Clayton, K. R. Knupp, E. Lenning, M. T. Friedlein, R. Castro, and E. S. Bentley, 2017: Analysis of mesovortex characteristics, behavior, and interactions during the second 30 June–1 July 2014 midwestern derecho event. Electronic *J. Severe Storms Meteor*., **12** (2), 1–33. [Available online at https://ejssm.org/ojs/index.php/ejssm/article/viewFile/162/111.]

Marion, G. R., and R. J. Trapp, 2021: Controls of quasi-linear convective system tornado intensity. *J. Atmos. Sci*., **78**, 1189–1205, Crossref.

Pfost, R. L., and A. E. Gerard, 1997: "Bookend vortex" induced tornadoes along the Natchez Trace. *Wea. Forecasting*, **12**, 572–580, Crossref.

Przybylinski, R. W., 1995: The bow echo: Observations, numerical simulations, and severe weather detection methods. *Wea. Forecasting*, **10**, 203–218, Crossref.

Rasmussen, E. N., and D. O. Blanchard, 1998: A baseline climatology of sounding-derived supercell and tornado forecast parameters. *Wea. Forecasting*, **13**, 1148–1164, Crossref.

Rotunno, R., and J. B. Klemp, and M. L. Weisman, 1988: A theory for strong, long-lived squall lines. *J. Atmos. Sci*., **45**, 463–485, Crossref.

Schaefer, J. T., 1990: The critical success index as an indicator of warning skill. *Wea. Forecasting*, **5**, 570–575, Crossref.

Schaumann, J. S., and R. W. Przybylinksi, 2012: Operational application of 0-3 km bulk shear vectors in assessing QLCS mesovortex and tornado potential. Preprints, *26th Conf on Severe Local Storms*, Nashville, TN, Amer. Meteor. Soc., P9.10. [Available online at https://ams.confex.com/ams/26SLS/webprogram/Paper212008.html.]

Sessa, M. F., and R. J. Trapp, 2020: Observed relationship between tornado intensity and pretornadic mesocyclone characteristics. *Wea. Forecasting*, **35**, 1243–1261, Crossref.

Skow, K. D., and C. Cogil, 2017: A high-resolution aerial survey and radar analysis of quasi-linear convective system surface vortex damage paths from 31 August 2014. *Wea. Forecasting*, **32**, 441–467, Crossref.

Smith, B. T., R. L. Thompson, J. S. Grams, C. Broyles, and H. E. Brooks, 2012: Convective modes for significant severe thunderstorms in the contiguous United States. Part I: Storm classification and climatology. *Wea. Forecasting*, **27**, 1114–1135, Crossref.

Smull, B. F., and R. A. Houze Jr., 1987: Rear inflow in squall lines with trailing stratiform precipitation. *Mon. Wea. Rev.*, **115**, 2869–2889, Crossref.

Thompson, R. L., B. T. Smith, J. S. Grams, A. R. Dean, and C. Broyles, 2012: Convective modes for significant severe thunderstorms in the contiguous United States. Part II: Supercell and QLCS tornado environments. *Wea. Forecasting*, **27**, 1136–1154, Crossref.

Trapp, R. J., E. D. Mitchell, G. A. Tipton, D. W. Effertz, A. I. Watson, D. L. Andra Jr., and M. A. Magsig, 1999: Descending and nondescending tornadic vortex signatures detected by WSR-88Ds. *Wea. Forecasting*, **14**, 625–639, Crossref.

____, S. A. Tessendorf, E. S. Godfrey, and H. E. Brooks, 2005: Tornadoes from squall lines and bow echoes. Part I: Climatological distribution. *Wea. Forecasting*, **20**, 23–34, Crossref.

Wakimoto, R. M., H. V. Murphey, C. A. Davis, and N. T. Atkins, 2006: High winds generated by bow echoes. Part II: The relationship between the mesovortices and damaging straight-line winds. *Mon. Wea. Rev.*, **134**, 2813–2829, Crossref.

WDTD, 2021: WOC severe: QLCS hazards, challenges, and warning Techniques. NOAA/NWS Warning Decision Training Division. [Available online at: https://training.weather.gov/wdtd/courses/woc/severe/storm-structures-hazards/storm-modes/qlcs/presentation_html5.html.]

Weisman, M. L., and R. J. Trapp, 2003: Low-level mesovorticies within squall lines and bow echoes. Part I: Overview and dependence on environmental shear. *Mon. Wea. Rev.*, **131**, 2779–2803, Crossref.

Wheatley, D. M., and R. J. Trapp, 2008: The effect of mesoscale heterogeneity on the genesis and structure of mesovortices within quasi-linear convective systems. *Mon. Wea. Rev*, **136**, 4220–4241, Crossref.